



# An investigation of semisolid Al7075 feedstock billet produced by a gas-assisted direct thermal method

Nur Azhani Abd Razak<sup>1</sup> · Asnul Hadi Ahmad<sup>1,2</sup> · Mohd Maarof Rashidi<sup>3</sup> · Sumsun Naher<sup>4</sup>

Received: 10 August 2020 / Accepted: 15 March 2021  
© Springer-Verlag London Ltd., part of Springer Nature 2021

## Abstract

Semisolid metal (SSM) processing is a forming process which occurs within solidus and liquidus temperatures, and it requires feedstock billets with spheroidal microstructures. In this paper, a novel gas-assisted direct thermal method (DTM) is proposed as a method to create feedstock billets with fine spheroidal microstructures. Effect of different combination parameters between pouring temperature and holding time during the gas-assisted DTM technique on the microstructure of aluminium alloy 7075 feedstock billets was investigated. Pouring of molten aluminium alloy 7075 was conducted at temperatures between 645 and 685 °C, while holding time was set between 20 and 60 s. The melt was cooled down within the semisolid temperature range in a cylindrical copper mould with the help of carbon dioxide (CO<sub>2</sub>) gas before quenching in room temperature water. Results revealed that the smallest primary phase grain size formed at the combination parameters of 645 °C pouring temperature and 20-s holding time. Furthermore, the same combination parameters also produced the highest circularity value. The addition of external CO<sub>2</sub> gas surrounded the copper mould as a rapid cooling agent was found to have a significant improvement of 36.4% to the formation of smaller primary grain and spheroidal structure. It is concluded that the lowest pouring temperature and shortest holding time coupled with rapid cooling condition from the addition of external CO<sub>2</sub> during DTM produced the finest and most globular structure of primary phase size.

**Keywords** Semisolid metal · Aluminium 7075 · Direct thermal method · Pouring temperature · Spheroidal microstructure

## 1 Introduction

In recent years, semisolid metal (SSM) processing is deemed as sophisticated technology and gains attention worldwide due to its ability to produce a higher quality of engineering parts but with lower cost [1, 2]. In contrast to conventional casting, this processing method occurs within the range of liquidus and solidus temperature. The fluidity or liquidity of

the molten metal can have substantial variations within this solidification region. As opposed to obtaining dendritic microstructures through conventional processing techniques, spheroidal or globular microstructures can be attained from SSM processing by controlling process parameters, for instance, cooling rate, stirring speed, stirring time, and stirring type [2–4]. The primary phase morphology of SSM slurries influenced the flow behaviour of SSM [5]. According to a previous study [6], poor flowability was often found in a molten metal having dendritic structures than equiaxed structures at the same solid fraction. It was due to the dendritic structures prone to engage with one another during the application of an external force, and thereby, hindered the flows of the material. On the contrary, spheroidal or globular structures produced higher flowability as their shape geometries allowed for better rotation, slip, and movement under a small external force [7, 8]. A finer microstructure displayed higher flowability as it could move freely with only fewer collisions between the particles and low viscosity [2, 8].

Near-net-shape components with excellent mechanical properties can be achieved by SSM processing [2, 3, 5, 9].

✉ Nur Azhani Abd Razak  
azhani@ump.edu.my

<sup>1</sup> Department of Mechanical Engineering, College of Engineering, Universiti Malaysia Pahang, Lebuhraya Tun Razak, 26300 Gambang, Kuantan, Pahang, Malaysia

<sup>2</sup> Centre for Automotive Engineering, Universiti Malaysia Pahang, 26600 Pekan, Pahang, Malaysia

<sup>3</sup> Faculty of Mechanical and Automotive Engineering Technology, Universiti Malaysia Pahang, 26600 Pekan, Pahang, Malaysia

<sup>4</sup> Department of Mechanical Engineering and Aeronautics, City University of London, London EC1V 0HB, UK

Thus, it is a sought-after process for creating components that have intricate part geometries. Moreover, it has another positive effect that is a reduction of gas entrapment. It is due to the effect of laminar flow inside the die cavity when conducting the SSM process. This has resulted in a production of high integrity components with uniform and fine microstructures. Furthermore, SSM processing also promotes the extension of die life due to reduction of thermal shock, and at the same time having fewer shrinkage porosity defect in comparison with other conventional processes [10, 11].

The key towards a successful SSM processing is to have a feedstock billet with spheroidal or globular microstructures. Over the past few years, a variety of processing methods have been created to develop spheroidal or globular microstructures in feedstock billets. The methods are categorized into three major categories that are the solid-state methods, liquid metal methods, and a combination of both methods [3, 9]. Although all the methods can produce feedstock billets with spheroidal microstructures, however, the direct thermal method is preferred as it is a simple method due to less equipment used and low processing costs [8, 12–14]. Through this method, spheroidal or globular microstructures in feedstock billet can be produced by pouring the low superheat of molten metal into a cylindrical mould that has high conductivity but very low thermal mass. The matching of heat between the molten metal and the cylindrical mould leads to a pseudo-isothermal arrest within the solidification region of the molten metal, due to the very low rate of heat dissipation to the surroundings [14]. Consequently, the spheroidal or globular microstructures are developed throughout the holding time and quenching in the room temperature water is subsequently done to retain the spheroidal or globular microstructures.

Due to the requirement of weight saving in the automotive and aerospace industries, aluminium alloys are regarded as one of the potential candidates for these applications. Die casting, permanent mould casting, and sand casting are typically used for manufacturing components of aluminium alloy. However, those processes are not possible to be utilized for the production of intricate and thin-walled aluminium alloy components in those industries. Therefore, precision castings such as expendable pattern shell casting [15–17] are found to be beneficial for the manufacturing of intricate and thin-walled aluminium alloy components. However, the microstructures of aluminium alloy components attained by the expendable pattern shell casting process produce a coarse dendrite with an inhomogeneous distribution which leads to a decreased in mechanical properties. Therefore, grain refinement is of great interest and several methods are employed to obtain finer grain structures such as chemical elements modification [18], mechanical vibration [15–17], ultrasonic vibration [19], and electromagnetic vibration [20].

On the other hand, SSM processing has opened up a way to produce near-net-shape components of aluminium alloy with

less energy consumption in comparison to the conventional casting process [21]. Although most studies are performed on aluminium-silicon alloy [1, 14, 22–27], however, the use of wrought aluminium alloy in SSM processing has seen an increase for the past few years [12, 28–32]. A study conducted by Ahmad et. al. [12] on AA7075 had proved a correlation among pouring temperature and holding time during DTM for spheroidal microstructure generation in the SSM feedstock billet. They mentioned that a combined pouring temperature of 660 °C and holding time of 60 s produced the most spheroidal or globular primary phase structures. Another study claimed that better spherical or globular structures were developed by a combination of lower pouring temperature and shorter holding time [33]. The increase in spheroidal or globular primary phase structures would enhance the flowability of the molten metal throughout SSM processing, and as a result, produced near-net-shape components with excellent mechanical properties. Therefore, it is important to control the processing parameters during SSM processing that affect the undercooling during solidification. This study emphasizes the process to increase the undercooling of the alloy using an innovative method of rapid cooling by adding an external cooling gas to the existing DTM process. This current work aims to examine the correlation among pouring temperature and holding time during DTM, coupled with rapid cooling by the CO<sub>2</sub> gas to develop spheroidal or globular microstructures for the SSM wrought aluminium alloy 7075 feedstock billet.

## 2 Experimental procedure

Commercial wrought aluminium alloy 7075 was used in this study. Optical Emission Spectroscopy, Foundry Master Oxford Instruments was calibrated before being used to determine the chemical composition of this alloy. Six chemical composition tests were conducted for better accuracy. The chemical composition of the alloy used in this study and those from the literature are shown in Table 1.

### 2.1 Gas-assisted direct thermal method experiment

A resistance-heated box furnace was used to heat a 1 kg of aluminium alloy 7075 ingot. The ingot was superheated to a temperature of 700 °C in a graphite crucible. Once the molten metal had achieved the desired temperature, it was then taken out from the furnace, and its temperature was measured. A 1-mm diameter of K-type thermocouple and a Graphtec GL-220 data logger were used to measure the temperature of molten metal prior to pouring it into a cylindrical copper mould with dimensions of 120 mm in height, 25 mm in diameter, and 1-mm wall thickness. The temperatures when pouring the molten metal into the cylindrical copper mould were set at an increment of 20 °C starting from 645 °C until 685 °C. The

**Table 1** Chemical composition of wrought aluminium 7075 alloys from the experiment and literature

Source (wt.%)	As-received sample	Ahmad et al [34]	Bäckerud et al [35]	ASM [36]
Al	89.8	88.5	Bal.	87.1–91.4
Cr	0.27	0.2	0.19	0.18–0.28
Cu	1.33	2.02	1.36	1.2–2.0
Fe	0.22	0.24	0.28	<0.5
Mg	2.26	2.38	2.49	2.1–2.9
Mn	0.05	0.12	-	<0.3
Si	0.16	0.14	0.11	<0.4
Ti	0.07	0.09	-	<0.2
Zn	5.74	6.04	-	5.1–6.1

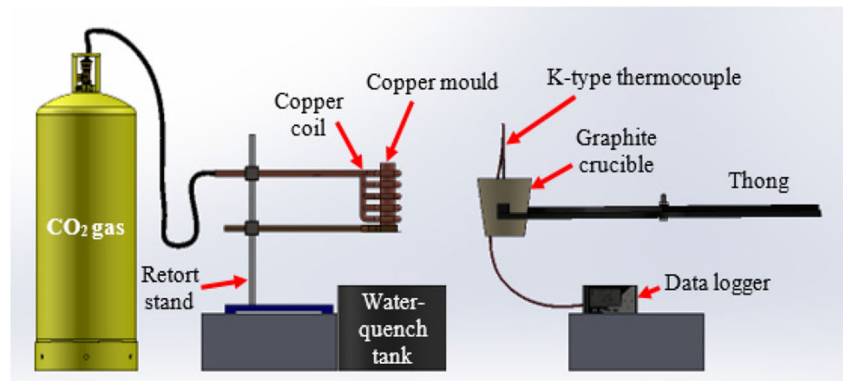
molten metal was kept in the copper mould for three different time intervals that were 20 s, 40 s, and 60 s. A CO<sub>2</sub> gas that acted as a rapid cooling agent surrounded the copper mould was provided simultaneously when pouring process of the molten metal began. Quenching in the water at room temperature was carried out once the melt had reached its desired holding time. Another sample termed as a reference sample was produced by having a pouring temperature of 685 °C and cooled inside the copper mould without quenching. This sample was viewed as experiencing normal solidification condition. The arrangement of the gas-assisted DTM experimental setup is shown in the following Fig. 1, and the parameters used during the experiment are tabulated in Table 2.

## 2.2 Metallographic sample preparation

The wrought aluminium alloy that had solidified was removed from the copper mould. The initial dimensions of the solidified alloy by the gas-assisted DTM was 120 mm in length and 25 mm in diameter. A linear precision sectioning machine was used to section about 5 mm from the top part of the gas-assisted DTM samples. Then, another 20 mm in length from the top of the samples were sectioned for metallographic observation. The remaining samples were set for mechanical testing to determine the mechanical properties.

Samples for metallographic observation were mounted with Bakelite thermoset phenolic resin before grinding process. Buehler Simplimet 1000 Mounting Press hot mounting machine was used to perform the mounting process. Appropriate parameters during mounting were chosen, which curing temperature set at 150 °C and duration was 1 min and followed by cooling off the sample for 3 min. Then, a Metkon Forcipol 2V grinding machine was used to grind the samples. The grinding wheel speed was set at 250 rpm, and the grinding process started with the order of 320-, 800-, 1200-, and 2400-grit size silicon carbide for 3 min. The samples were then polished by using a separate polishing cloth for 6- and 3- $\mu$ m size diamond suspension and followed by another polishing cloth with 1- $\mu$ m size diamond suspension. All the polishing process by diamond suspension were conducted at the polishing speed of 150 rpm for 5 min at each stage. The samples were finally polished with 0.05- $\mu$ m size colloidal silica suspension by using a different polishing cloth. Finally, Keller's reagent was used to etch the polished samples for approximately 30 s [37] to expose the grain boundaries of the material for microscopic observation. Both Olympus BX53M optical microscope and Motic Images Plus 3.0 ML software were used to view and capture the microstructure images.

Image J software was chosen as an analysis tool to determine the primary phase diameter, circularity, and aspect ratio

**Fig. 1** Arrangement of gas-assisted DTM experimental setup

**Table 2** Processing parameters during gas-assisted DTM experiment

Sample no.	Pouring temperature (°C)	Holding time (s)
1	685	60
2		40
3		20
4	665	60
5		40
6		20
7	645	60
8		40
9		20
10	685	Without quenching

measurement. Circularity is a measure of closeness of shape to an ideal circle which forms in a microstructure, and the range is in between 0.0 and 1.0. As the value approaches 1.0, the shape is deemed as having a perfect circular shape. On the other hand, as the value decreases toward 0.0, the shape becomes more elongated. Aspect ratio is an indicator for a shape having either circular or square morphology. The higher the value of aspect ratio, the more elongated the particle is. The following Eq. (1) and Eq. (2) provide the calculation method for circularity,  $C$ , and aspect ratio,  $AR$ .  $P$  and  $A$  in Eq. (1) correspond to a perimeter and an area of the particle, respectively:

$$C = 4\pi \left( \frac{A}{P^2} \right) \quad (1)$$

$$AR = \frac{\text{major axis}}{\text{minor axis}} \quad (2)$$

### 3 Results and discussion

Thermal analysis of the wrought aluminium alloy 7075 used in this study was conducted in a separate work [38]. Based on the study, the liquidus temperature occurred at a temperature of 619.30 °C, while the solidus temperature happened at 421.90 °C. This information is used to determine the processing parameters during the gas-assisted direct thermal method.

Formation of microstructure in each sample of gas-assisted DTM was analyzed to decipher the influence of both processing parameters which were pouring temperature and holding time. Figures 2, 3, and 4 show the microstructure for a combination of pouring temperature of 685 °C, 665 °C, and 645 °C with holding time of 60 s, 40 s, and 20 s, respectively. Similarly, microstructure formation in sample 10 which was produced at a pouring temperature of 685 °C and solidified without quenching process is shown in Fig. 5.

The purpose of holding time in gas-assisted DTM was to provide a sufficient temperature needed prior to quenching. Based on a previous study, the temperature drop inside the copper mould was recorded at 1.0 °C/s [12]. Therefore, the temperature of the molten metal in the copper mould before quenching was approximately calculated. It was found that the molten metal temperatures before quenching for sample 1, sample 2, and sample 3 were 625 °C, 645 °C, and 665 °C, respectively. The molten metal temperatures before quenching for sample 4, sample 5, and sample 6 were estimated to be 605 °C, 625 °C, and 645 °C, whereby the calculated molten metal temperatures for sample 7, sample 8, and sample 9 before quenching were at 585 °C, 605 °C, and 625 °C, respectively.

Analysis of the micrograph in Figs. 2, 3, 4, and 5 revealed a significant difference in microstructure evolution between all

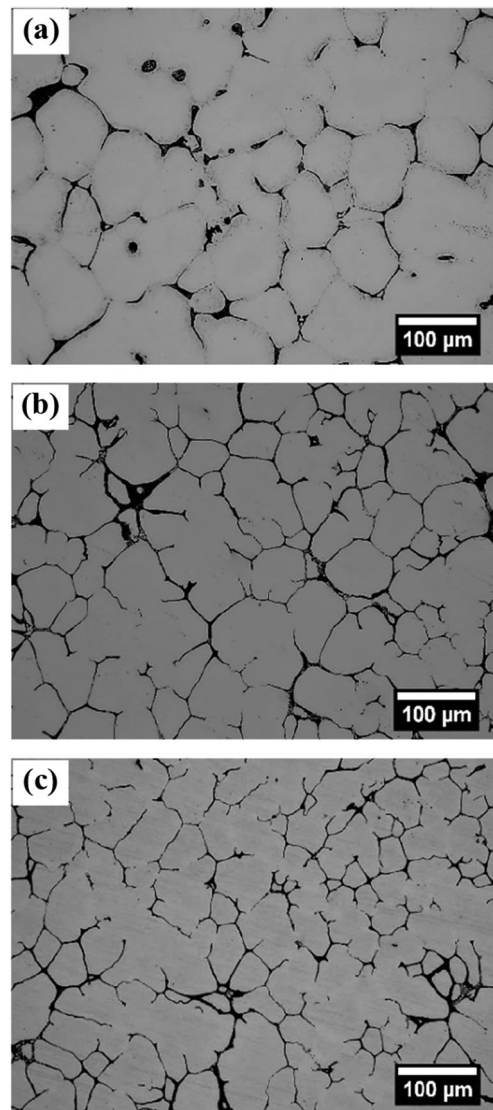


**Fig. 2** Microstructure at the centre of feedstock billet of **a** sample 1, **b** sample 2, and **c** sample 3

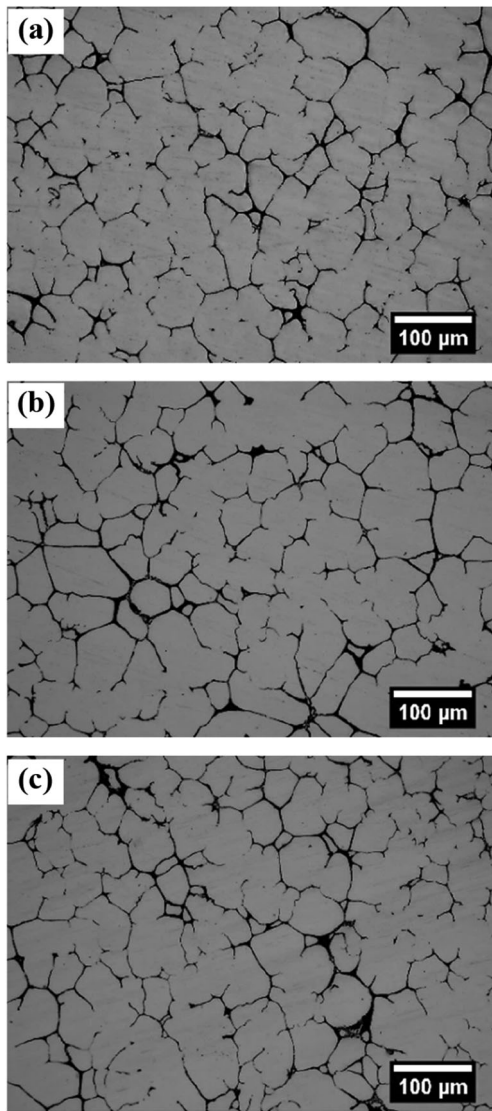


**Fig. 3** Microstructure at the centre of feedstock billet of **a** sample 4, **b** sample 5, and **c** sample 6

samples which were quenched at various time intervals. Furthermore, the most prominent finding was found in sample 10 which was poured at a temperature of 685 °C and solidified in the copper mould without quenching. The grain size of sample 10 was larger in comparison to other samples. The difference is apparent between sample 1 and sample 10 as depicted in Figs. 2a and 5.

Aside from qualitative measurement made by micrograph observation, a quantitative measurement which is grain size measurement was carried out to provide more precise and accurate analysis of the microstructure evolution in all samples. Three different categories of grain size measurement were performed, which were the average values for the primary phase grain diameter, circularity, and aspect ratio. Figures 6, 7, and 8 show the results of the grain size measurement for the categories described above. A significant

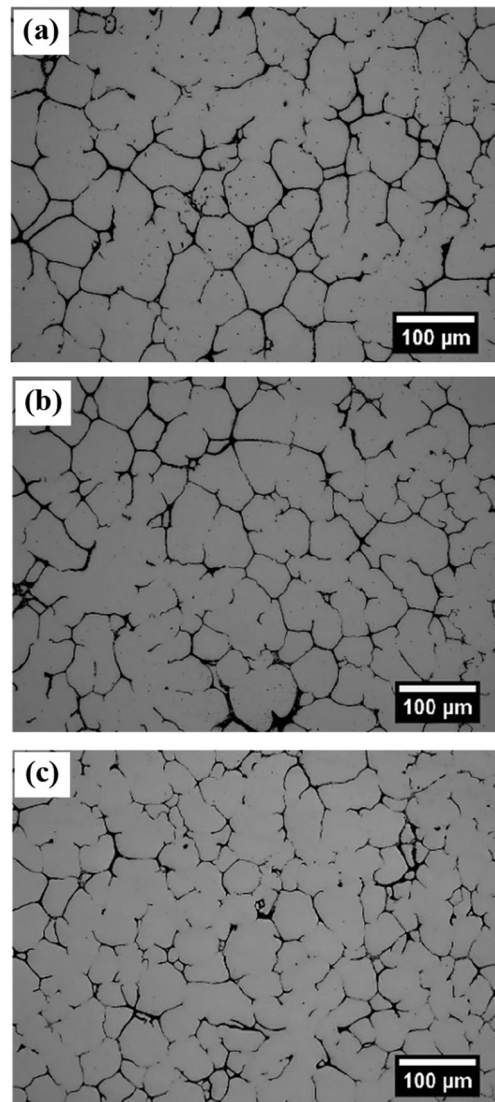


**Fig. 4** Microstructure at the centre of feedstock billet of **a** sample 7, **b** sample 8, and **c** sample 9

variation was noticed between the average primary phase grain diameters for samples 1, 2, and 3, which are illustrated in Fig. 6. Furthermore, sample 10, which had solidified in the

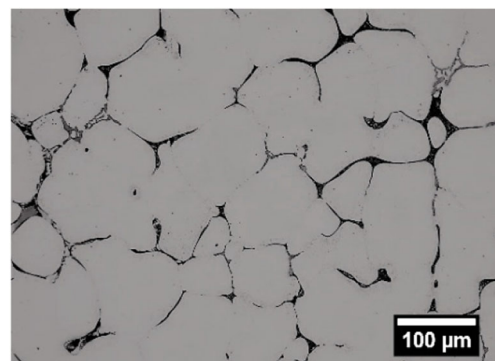


**Fig. 5** Microstructure at the centre of feedstock billet of sample 10

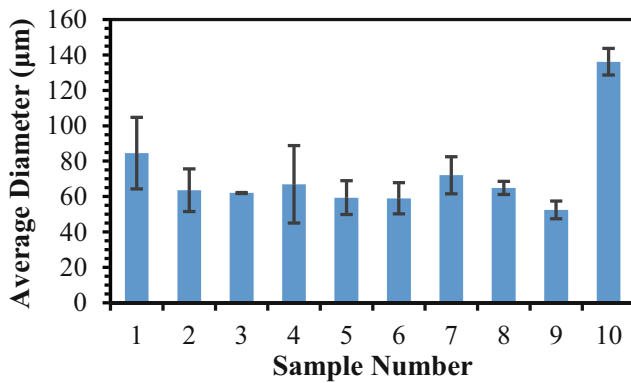


**Fig. 6** Measurement of average primary phase grain diameter for 10 samples with errors having 95% confidence intervals

copper mould without quenching, also showed an evident variation from the other samples. It recorded the maximum value of the average primary grain diameter, which was 136.18 µm. This is a sign of the bigger or larger size structures that exist within sample 10. Conversely, sample 9, which had a pouring temperature of 645 °C and holding time of 20 s produced the finest primary grain structure of 52.40 µm. Other than that, the analysis of circularity was also performed on the microstructure evolution of each sample. Figure 7 illustrates the circularity value of microstructure for each sample. The highest circularity value was observed in sample 9, having the lowest of both pouring temperature and holding time. It indicated that lower pouring temperature was an important factor for the evolution of finer and more globular or spheroidal microstructures. Previous findings by several researchers also recorded the same output [23, 33, 39]. Moreover, pouring temperature is associated with the cooling rate during the gas-assisted DTM process. Lower pouring temperature results in a higher cooling rate. It was due to less superheat to be dissipated from the molten metal in the copper mould to the surrounding. The low pouring temperature in this study had resulted in finer grain size and more globular microstructures due to the rise of cooling rate. It was proven by

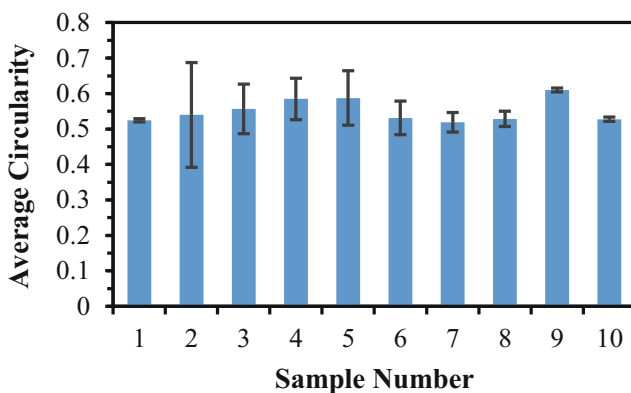


**Fig. 7** Measurement of average microstructure circularity for 10 samples with errors having 95% confidence intervals

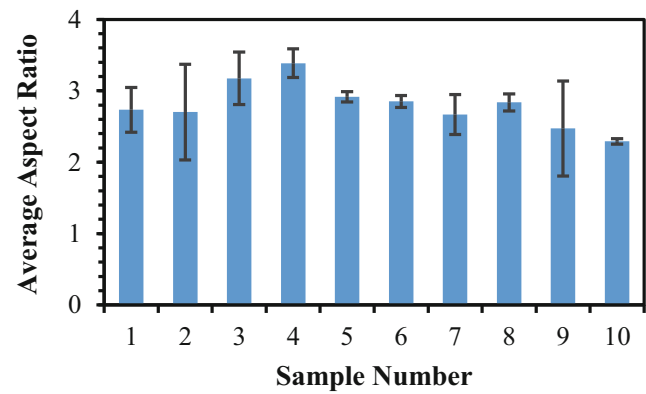


**Fig. 8** Measurement of average microstructure aspect ratio for 10 samples with errors having 95% confidence intervals

the analysis between sample 3 and sample 9. Sample 9 which was poured at 645 °C had a smaller primary grain diameter but a higher value of circularity than sample 3. The lower the pouring temperature, the higher the cooling rate because a shorter time required to dissipate the heat from above to below the liquidus temperature.

Correlation between pouring temperature and microstructure evolution was controlled by the undercooling temperature happened during solidification [40]. The undercooling is manipulated by the solidification rates, which is controlled by the mould thickness and mould material used. Hence, microstructure evolution is governed by the amount of undercooling. The higher the cooling rate, the larger the undercooling is. The raise in undercooling enhances the nucleation activity, which in turn, results in a finer grain microstructure. Therefore, a finer grain and spheroidal microstructure produced within a sample are due to the higher cooling rate happened during solidification. The success of having a smaller primary phase and spheroidal microstructure by the DTM was depended on the cooling rate [41, 42]. The theory of gas-assisted DTM, which permits for a rapid change of heat impedes the microstructure evolution. The copper mould and the external CO<sub>2</sub> gas which surrounded the copper mould provided a chilling effect which produced a finer size of nuclei and influenced the spheroidal microstructure evolution. According to a previous study [43], the suitable primary grain structure in thixoforming feedstock billets was observed approximately around 100 µm. Based on the results, only sample 10 was not fit to be used for thixoforming process.

Furthermore, this study also revealed that the addition of external CO<sub>2</sub> gas applied to surround the copper mould has resulted in finer primary grain structure than the samples produced by the direct thermal method as shown in Fig. 9. The smallest average primary grain diameter for this study was found to be 52.4 µm, while the results without external cooling gas was 82.4 µm. This finding clearly showed that the addition of external cooling gas surrounding the copper mould has a significant improvement to the DTM process in

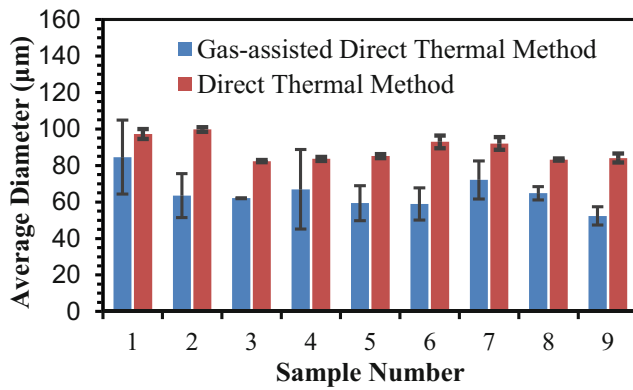


**Fig. 9** Comparison between average primary phase grain diameter for gas-assisted direct thermal method and direct thermal method samples with errors having 95% confidence intervals

providing smaller grain structures by 36.4%. The concept of having external CO<sub>2</sub> gas applied to surround the copper mould in the direct thermal method was similar to the application of water circulation underneath the inclined plate in cooling slope method. The water circulation in cooling slope method provides higher heat dissipation through convection to the surrounding, leading to the formation of more solid nuclei that results in finer grain size [44]. The same scenario happens in the gas-assisted direct thermal method. The external CO<sub>2</sub> gas has catalyzed more formation of solid nuclei happens in the melt, which was close to the mould wall. This action was due to the mould wall becomes the coldest surface as compared to other areas in the melt, resulted in the heat transfer from the hot to the cold zones. The CO<sub>2</sub> gas applied at the outer surface of the copper mould has increased the cooling action and therefore, improved the heat dissipation from the molten metal to the surrounding. The degree of undercooling becomes higher as more heat loss was recorded because of the cooling action provided by the CO<sub>2</sub> gas. Higher undercooling during solidification leads to more formation of solid nuclei, which resulted in a finer grain size because of a large number of grains per unit volume. Thus, it was proven that this innovative method of rapid cooling by adding external CO<sub>2</sub> gas surrounded the copper mould had increased the degree of undercooling, which in turn resulted in the formation of finer primary grain structure.

## 4 Conclusions

The experimental work revealed that a proper combination of pouring temperature and holding time was able to generate smaller and spheroidal primary grain structures. Combination of lower pouring temperature and shorter holding time led to the formation of a smaller size and spheroidal microstructure due to the higher cooling rate. The addition of external CO<sub>2</sub> gas surrounded the copper mould as a rapid

cooling agent was found to have a significant improvement of 36.4% to the formation of smaller primary phase grain and globular structure. It is summarized that the combined effect of 645 °C pouring temperature and 20-s holding time, coupled with the addition of CO<sub>2</sub> during DTM, produced finer and globular microstructure features for the wrought aluminium alloy 7075 feedstock billets suitable for SSM forming. The findings presented in this research contribute to details information and understanding regarding the behaviours of the Al7075 processed by gas-assisted DTM for thixoforming.

**Author contribution** Nur Azhani Abd Razak was in charge of the manuscript preparation, collecting data of the microstructure formation, and analysis of the microstructure results. Asnul Hadi Ahmad handled the feedstock billet production and analysis of the microstructure results. Mohd Rashidi Maarof prepared the metallographic samples, and Sumsun Naher was in charge of writing the introduction part of this manuscript and proofreading the manuscript.

**Funding** This study was funded by Universiti Malaysia Pahang and Centre for Automotive Engineering, Universiti Malaysia Pahang (RDU160311 and RDU1603125). Recipient: Asnul Hadi Ahmad.

**Availability of data and materials** Not applicable.

## Declarations

**Ethical approval** This manuscript does not contain any studies with human participants or animals performed by any of the authors.

**Consent to participate** Not applicable.

**Consent for publication** Not applicable.

**Competing interests** The authors declare no competing interests.

## References

- Kolahdooz A, Nourouzi S, Jooybari MB, Hosseinipour SJ (2016) Experimental investigation of the effect of temperature in semisolid casting using cooling slope method. *Proc Inst Mech Eng Part E J Process Mech Eng* 230:1–10
- Fan Z (2002) Semisolid metal processing. *Int Mater Rev* 47:49–85
- Atkinson HV (2010) Semisolid processing of metallic materials. *Mater Sci Technol* 26:1401–1413
- Atkinson HV (2005) Modelling the semisolid processing of metallic alloys. *Prog Mater Sci* 50:341–412
- Flemings MC (1991) Behavior of Metal Alloys in the Semisolid State. *Metall Trans A* 22A:957–981
- Lashkari O, Ghomashchi R (2007) The implication of rheology in semisolid metal processes: an overview. *J Mater Process Technol* 182:229–240
- Spencer DB, Mehrabian R, Flemings MC (1972) Rheological behavior of Sn-15 pct Pb in the crystallization range. *Metall Trans* 3: 1925–1932
- Brabazon D, Browne DJ, Carr AJ (2002) Mechanical stir casting of aluminium alloys from the mushy state: process, microstructure and mechanical properties. *Mater Sci Eng A* 326:370–381

9. Ahmad AH, Naher S, Aqida SN, Brabazon D (2014) Routes to spheroidal starting material for semisolid metal processing. In: Hashmi S, Van Tyne CJ, Batalha GF et al (eds) *Comprehensive Materials Processing*. First. Elsevier, Ltd., Oxford, UK, pp 135–148
10. Kirkwood DH (1994) Semisolid metal processing. *Int Mater Rev* 47:173–189
11. McLelland ARA, Henderson NG, Atkinson HV, Kirkwood DH (1997) Anomalous rheological behaviour of semisolid alloy slurries at low shear rates. *Mater Sci Eng A* 232:110–118
12. Ahmad AH, Naher S, Brabazon D (2014) Direct Thermal Method of Aluminium 7075. *Adv Mater Res* 939:400–408
13. Brabazon D, Browne DJ, Carr AJ (2003) Experimental investigation of the transient and steady state rheological behaviour of Al-Si alloys in the mushy state. *Mater Sci Eng A* 356:69–80
14. Browne DJ, Hussey MJ, Carr AJ, Brabazon D (2003) Direct thermal method: new process for development of globular alloy microstructure. *Int J Cast Met Res* 16:418–426
15. Jiang W, Fan Z, Liu D, Liao D, Dong X, Zong X (2013) Correlation of microstructure with mechanical properties and fracture behavior of A356-T6 aluminum alloy fabricated by expendable pattern shell casting with vacuum and low-pressure, gravity casting and lost foam casting. *Mater Sci Eng A* 560:396–403
16. Jiang W, Chen X, Wang B, Fan Z, Wu H (2016) Effects of vibration frequency on microstructure, mechanical properties, and fracture behavior of A356 aluminum alloy obtained by expendable pattern shell casting. *Int J Adv Manuf Technol* 83:167–175
17. Jiang W, Fan Z, Chen X, Wang B, Wu H (2014) Combined effects of mechanical vibration and wall thickness on microstructure and mechanical properties of A356 aluminum alloy produced by expendable pattern shell casting. *Mater Sci Eng A* 619:228–237
18. Kaur P, Dwivedi DK, Pathak PM (2012) Effects of electromagnetic stirring and rare earth compounds on the microstructure and mechanical properties of hypereutectic Al-Si alloys. *Int J Adv Manuf Technol* 63:415–420
19. Khosro Aghayani M, Niroumand B (2011) Effects of ultrasonic treatment on microstructure and tensile strength of AZ91 magnesium alloy. *J Alloys Compd* 509:114–122
20. Li M, Tamura T, Omura N, Miwa K (2009) Effects of magnetic field and electric current on the solidification of AZ91D magnesium alloys using an electromagnetic vibration technique. *J Alloys Compd* 487:187–193
21. Kenney MP, Courtois RD, Evans GM, Farior CP, Koch AA, Young KP (1998) Semi solid metal casting and forging. In: *Metals handbook*, 9th edn. ASM International, Materials Park, Ohio, USA, pp 327–338
22. Yang XR, Mao WM, Pei S (2007) Preparation of semisolid A356 alloy feedstock cast through vertical pipe. *Mater Sci Technol* 23:1049–1053
23. Ning ZL, Wang H, Sun JF (2010) Deformation behavior of semisolid A356 alloy prepared by low temperature pouring. *Mater Manuf Process* 25:648–653
24. Jarfors AEW (2004) Melting and coarsening of A356 during preheating for semisolid forming. *Int J Cast Met Res* 17:229–237
25. El-Mahallawi I, Shash Y (2010) Influence of nanodispersions on strength–ductility properties of semisolid cast A356 Al alloy. *Mater Sci Technol* 26:1226–1231
26. Forn A, Vaneetveld G, Pierret JC, Menargues S, Baile MT, Campillo M, Rassili A (2010) Thixoextrusion of A357 aluminium alloy. *Trans Nonferrous Met Soc China (English Ed)* 20:s1005–s1009
27. Birol Y (2007) A357 thixoforming feedstock produced by cooling slope casting. *J Mater Process Technol* 186:94–101
28. Ahmad AH, Naher S, Brabazon D (2014) Injection tests and effect on microstructure and properties of aluminium 7075 direct thermal method feedstock billets. *Key Eng Mater* 611–612:1637–1644
29. Ahmad AH, Naher S, Brabazon D (2015) Mechanical properties of thixoformed 7075 feedstock produced via the direct thermal method. *Key Eng Mater* 651–653:1569–1574
30. Lee S-Y, Oh S-I (2002) Thixoforming characteristics of thermomechanically treated AA 6061 alloy for suspension parts of electric vehicles. *J Mater Process Technol* 130:587–593
31. Zhang XZ, Chen TJ, Chen YS, Wang YJ, Qin H (2016) Effects of solution treatment on microstructure and mechanical properties of powder thixoforming 6061 aluminum alloy. *Mater Sci Eng A* 662:214–226
32. Li M, Li YD, Zheng HQ, Huang XF, Chen TJ, Ying MA (2018) Solidification behavior of 6061 wrought aluminum alloy during rheo-diecasting process with self-inoculation method. *Trans Nonferrous Met Soc China (English Ed)* 28:879–889
33. Ahmad AH, Naher S, Brabazon D (2014) The effect of direct thermal method, temperature and time on microstructure of a cast aluminum alloy. *Mater Manuf Process* 29:134–139
34. Ahmad AH, Naher S, Brabazon D (2013) Thermal profiles and fraction solid of aluminium 7075 at different cooling rate conditions. *Key Eng Mater* 554–557:582–595
35. Bäckerud L, Król E, Tamminen J (1986) *Solidification characteristics of aluminium alloys; volume 1: wrought alloys*. Skan Aluminium, Oslo
36. ASM International (1990) *ASM Metals Handbook, Properties and selection: nonferrous alloys and special-purpose materials*, Tenth. ASM International, Materials Park, OH
37. ASM International (2004) *ASM Handbook Volume 9 : Metallography and microstructures*. ASM International, Materials Park, OH
38. Razak NA, Ahmad AH, Rashidi MM (2020) Thermal profile and microstructure of wrought aluminium 7075 for semisolid metal processing. *Int J Automot Mech Eng* 17:7842–7850
39. Wang H, Li B, Jie J, Wei Z (2011) Influence of thermal rate treatment and low temperature pouring on microstructure and tensile properties of AlSi7Mg alloy. *Mater Des* 32:2992–2996
40. Gowri S, Samuel FH (1992) Effect of cooling rate on the solidification behavior of Al-7 Pct Si-SiCp metal-matrix composites. *Metall Trans A* 23:3369–3376
41. Zeer GM, Pervukhin MV, Zelenkova EG (2011) Effect of cooling rate on microstructure formation during crystallization of aluminum alloy 1417M. *Met Sci Heat Treat* 53:210–212
42. Hosseini VA, Shabestari SG, Gholizadeh R (2013) Study on the effect of cooling rate on the solidification parameters, microstructure, and mechanical properties of LM13 alloy using cooling curve thermal analysis technique. *Mater Des* 50:7–14
43. Atkinson HV, Burke K, Vaneetveld G (2008) Recrystallisation in the Semi-Solid State in 7075 Aluminium Alloy. *Mater Sci Eng A* 490:266–276
44. El-Mahallawi ISED, Mahmoud TS, Gaafer AM, Mahmoud FH (2015) Effect of pouring temperature and water cooling on the thixotropic semi-solid microstructure of A319 aluminium cast alloy. *Mater Res* 18:170–176

**Publisher's note** Springer Nature remains neutral with regard to jurisdictional claims in published maps and institutional affiliations.